# Auxiliary-cavity-assisted ground-state cooling of an optically levitated nanosphere in the unresolved-sideband regime

Jin-Shan Feng,[1] Lei Tan,[1,*] Huai-Qiang Gu,[2] and Wu-Ming Liu[3]

[1]*Institute of Theoretical Physics, Lanzhou University, Lanzhou 730000, China*

[2]*School of Nuclear Science and Technology, Lanzhou University, Lanzhou 730000, China*

[3]*Beijing National Laboratory for Condensed Matter Physics, Institute of Physics, Chinese Academy of Sciences, Beijing 100190, China*

We theoretically analyze the ground-state cooling of an optically levitated nanosphere in the unresolved-sideband regime by introducing a coupled high-quality-factor cavity. On account of the quantum interference stemming from the presence of the coupled cavity, the spectral density of the optical force exerting on the nanosphere gets changed and then the symmetry between the heating and the cooling processes is broken. Through adjusting the detuning of a strong-dissipative cavity mode, one obtains an enhanced net cooling rate for the nanosphere. It is illustrated that the ground-state cooling can be realized in the unresolved sideband regime even if the effective optomechanical coupling is weaker than the frequency of the nanosphere, which can be understood by the picture that the effective interplay of the nanosphere and the auxiliary cavity mode brings the system back to an effective resolved regime. Besides, the coupled cavity refines the dynamical stability of the system.

## I. INTRODUCTION

Cavity optomechanics, providing the effective coupling between light and mesoscale matter, has been of interest in theoretical and experimental investigations [1–6]. As an implementation of cavity optomechanics, optically levitated nanosphere [7–11] in cavity is an important platform for realizing the quantum behavior at macroscale and exploring new applications of this field. The lack of the mechanical support in such levitated system leads to high mechanical quality factor and long coherence time. These benefits make the system have prominent advantages in ultrasensitive measurement [12–24] and tests of fundamental theories that include nonlinear [25–32], nonequilibrium [33,34], macroscopic quantum behavior [35–40], Brownian motion [41,42], and other aspects [43–48]. Although remarkable advances have been seen for the levitated nanosphere system, many related studies and highly sensitive measurements are still limited by the thermal noise. So it is a prior condition for all work to cool the nanosphere [49–58] as a micromechanical resonator all the way to quantum ground state.

The cooling utilizing radiation pressure of levitated nanosphere in a cavity [59–62] is based on the principle that the scattering process related to cooling (anti-Stokes process) can be enhanced by choosing appropriate detuning between driving field and the cavity mode [63]. This requires the levitated nanosphere system to be in the "resolved-sideband" regime, where the cavity linewidth should be smaller than the mechanical oscillator resonance frequency. Such requirement is stringent for the levitated nanosphere system characterized by low oscillation frequency ($<1$ MHz) with large cavity decay. On the other hand, a low-frequency nanosphere has large zero-point motion, and methods for cooling such a nanosphere to the quantum regime are beneficial to new technical applications as well as fundamental studies. To relax

this limitation, there have been several specific proposals, such as the dissipative coupling mechanism [64–68], parameter modulations [69–72], and hybrid system approaches [73–94], to achieve the ground-state cooling in unresolved-sideband regime [95,96] for the cavity optomechanical system.

In this paper, we couple an additional high-$Q$ cavity to a single optomechanical cavity with a levitated nanosphere. This system has its own advantages over the hybrid optomechanical system with macroscopical quantum system, such as superconduction, BEC, two-level atomic ensembles, etc. Easy engineering of high-$Q$ cavity [97,98], fixed position, and room-temperature quantum optomechanics [7] make it more practical and scalable. Furthermore, the parameters of the optical and the mechanical properties can be optimized individually in this system. Besides, contrary to traditional all-optical domain single cavity cooling, this proposal solves the deficiency that one can realize ground-state cooling for a lower-frequency resonator in the high-$Q$ cavity with very low cooling efficiency. We study the state cooling of nanosphere in the unresolved-sideband regime. It is shown that the destructive quantum interference behavior in the optical force spectrum changes the symmetry between the cooling and the heating processes of the nanosphere. For our model, the ground-state cooling can be achieved in larger optomechanical cavity decay rate under the condition that the effective coupling between the cooling field and the nanosphere is weaker than the frequency of the nanosphere. This condition is different from the relevant research in extremely strong optomechanical coupling. To comprehend this result and the novel phenomena in the cooling process of nanosphere, an effective indirect coupling between the auxiliary cavity and the nanosphere is derived. By the effective parameters in the indirect coupling regime, it is demonstrated that the existence of the auxiliary cavity can improve the dynamical stability of the cooling system.

As the auxiliary cavity is added, the interactions in our system become richer than a single cavity in all-optical domain system. These tanglesome interactions give rise to

---

*tanlei@lzu.edu.cn

new physical phenomena, such as entanglement without direct coupling [99], state transfer [100], and mechanical squeezing [101], which inevitably appear in the network constituted of a coupled optomechanical system. Thus our system is a good platform for studying the quantum effects in two-coupled-cavity system. The paper is organized as follows. In Sec. II we describe the Hamiltonian of the system and in Sec. III we derive the quantum Langevin equations for the system operators. Section IV is devoted to the analysis of cooling of the nanosphere. The coherence coupling and the dynamical stability of this system will be discussed in Sec. V, followed by the conclusion of our work in Sec. VI.

## II. MODEL HAMILTONIAN

The system we consider includes two coupled cavities, as shown in Fig. 1. The first one provides a simple cavity-optomechanical system, of which the mechanical part is formed by an optically levitated nanosphere [7]. The dielectric nanosphere is manipulated by two spatial modes of this cavity. It is confined to an optical dipole trap [102] provided by mode 1 which is driven resonantly. When the radius of the nanosphere is far smaller than the wavelength of this mode, the nanosphere can be treated as a point dipole and the dipole trap is well approximated to a harmonic trap for the range of motion of the nanosphere [7]. So the dynamics of the nanosphere is equivalent to a resonator. Mode 2 is driven by a weaker beam and provides a radiation pressure for cooling the motion of the nanosphere. Under the premise of the resonator approximation, the mutual effect of this mode and the nanosphere is parallel to the effect of radiation pressure on a moving mirror in Fabry-Pérot cavity [1,7]. In a real experiment, the motion of the nanosphere is strictly limited in one dimension by the corresponding technical approach [41,49]. The second cavity supports an auxiliary field (denoted mode 3), which does not interact with the nanosphere. The coupling between two cavities is realized by the hopping through the joint mirror of photons in them [103–111]. They are driven by the corresponding pump laser. In what follows, we refer to them as optomechanical cavity and auxiliary cavity,
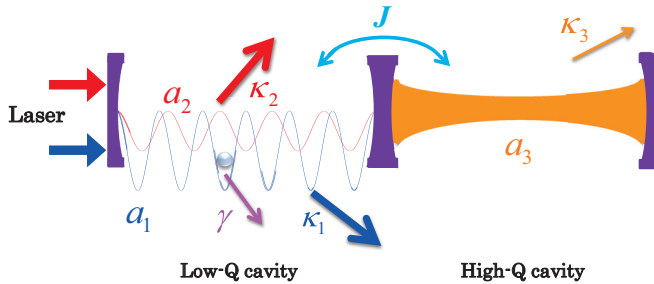


FIG. 1. Hybrid optomechanical setup containing three fixed mirrors and one optically levitated nanosphere. The left mirror, the nanosphere, and the left part of the middle mirror constitute a cavity-optomechanics system. The cavity has a low $Q$. The second quantum cavity is formed by the right part of the middle mirror and the right mirror, which has a high $Q$ and doesn't interact with the levitated nanosphere. These two cavities are coupled by the tunneling of cavity fields through the middle mirror.

respectively. The Hamiltonian of the system is given in a rotating frame (with $\hbar = 1$) by [7,96]

$$
\begin{aligned}
\hat{H} = & -\Delta_1 \hat{a}_1^\dagger \hat{a}_1 - \Delta_2 \hat{a}_2^\dagger \hat{a}_2 - \Delta_3 \hat{a}_3^\dagger \hat{a}_3 + \frac{\hat{p}^2}{2m} - g_1 \hat{a}_1^\dagger \hat{a}_1 (\cos 2k_1 \hat{x} - 1) \\
& - g_2 \hat{a}_2^\dagger \hat{a}_2 \cos 2\left( k_2 \hat{x} - \frac{\pi}{4} \right) + J \hat{a}_2^\dagger \hat{a}_3 + J^* \hat{a}_3^\dagger \hat{a}_2 \\
& + (E_1^* \hat{a}_1 + E_1 \hat{a}_1^\dagger) + (E_2^* \hat{a}_2 + E_2 \hat{a}_2^\dagger) + (E_3^* \hat{a}_3 + E_3 \hat{a}_3^\dagger).
\end{aligned}
\tag{2.1}
$$

The first line represents the free Hamiltonian of the system, where $\Delta_1 = \omega_1 - \omega_o$, $\Delta_2 = \omega_2 - \omega_o$, and $\Delta_3 = \omega_3 - \omega_a$ are the detunings between the driving field and cavity mode frequencies. $\omega_{i(i=1,2,3)}$, $\omega_o$, and $\omega_a$ correspond to the pump fields, optomechanical cavity mode, and auxiliary cavity mode frequencies, respectively. $\hat{a}_{i(i=1,2,3)}$ is the annihilation operator for the corresponding cavity mode, $\hat{p}$ is the momentum operator of the center of mass of the nanosphere, and $m$ is the mass of the nanosphere.

The interactions are described by the second line. The previous two terms correspond to the optomechanical coupling of optical modes $\hat{a}_{1,2}$ with the center-of-mass motion of the nanosphere. $g_{i(i=1,2)} = \frac{3V}{4V_{c,i}} \frac{\epsilon - 1}{\epsilon + 2} \omega_i$ quantifies the optomechanical interaction strength, where $V$ and $V_{c,i}$ are the nanosphere and the corresponding optical mode volumes, $\epsilon$ is the dielectric constant of the nanosphere, and $\hat{x}$ is the center-of-mass position operator of the nanosphere [7]. The two remaining terms stand for the interplay between optomechanical and auxiliary cavity modes. The terms mean that, when the photons of mode 3 in the auxiliary cavity tunnel into the optomechanical, the photons immediately become mode 2 without any relationship to the auxiliary cavity. The auxiliary cavity cannot directly couple the nanosphere. The tunnel-coupling strength of the cavities is characterized by the parameter $J$. This parameter is a phenomenological constant. The explicit value for $J$ depends on the specifics of the experimental setup, especially the material property of the joint mirror and the mode matching of the coupling fields. So it is cumbersome to give an accurate expression for the explicit value. A reasonable method without losing physical essence is that we neglect the loss stemming from the material property and assume the mode matching is perfect. Because the input and output at the two sides of the joint mirror are equal when the system attains steady, one can get $J = \sqrt{\kappa_2 \kappa_3}$ [81,112]. It needs to be emphasized that the photons of node 1 inevitably tunnel to the auxiliary cavity through the joint mirror. So the coupling between modes 1 and 3 is always present. Due to this mode matching, the photons from mode 1 can rarely tunnel to the auxiliary cavity, and the dynamics of mode 3 has hardly any change. We can safely omit the tunneling of node 3.

The last line accounts for the optical driving, with $E_{i(i=1,2,3)} = \sqrt{\kappa_i^{\text{ex}} P_i / \hbar \omega_i} e^{i\phi_i}$ the amplitudes of pump lasers, $P_{i(i=1,2,3)}$ the input powers, $\kappa_{i(i=1,2,3)}^{\text{ex}}$ the decay rates of the photons into the associated outgoing mode, and $\phi_{i(i=1,2,3)}$ the initial phases for the input lasers [96].

Based on the fact that $\omega_1, \omega_2 \gg |\omega_1 - \omega_2|$, for simplicity, we assume that modes 1 and 2 have semblable properties, so $\omega_1 \approx \omega_2 = \omega$, etc.

## III. HEISENBERG MOTION EQUATION AND LINEARIZATION

From the Hamiltonian given by Eq. (2.1), we obtain the Heisenberg-Langevin equations of the system operators:

$$\dot{a}_1 = \left(i\Delta_1 - \frac{\kappa}{2}\right)\hat{a}_1 - iE_1 + \sqrt{\kappa}\hat{a}_{\text{in},1},$$

$$\dot{a}_2 = \left[i(\Delta_2 + 2gk\hat{x}) - \frac{\kappa}{2}\right]\hat{a}_2 - iJ\hat{a}_3 - iE_2 + \sqrt{\kappa}\hat{a}_{\text{in},2},$$

$$\dot{a}_3 = \left(i\Delta_3 - \frac{\kappa_3}{2}\right)\hat{a}_3 - iJ^*\hat{a}_2 - iE_3 + \sqrt{\kappa_3}\hat{a}_{\text{in},3},$$

$$\dot{p} = -4gk^2\hat{a}_1^\dagger\hat{a}_1\hat{x} + 2gk\hat{a}_2^\dagger\hat{a}_2 - \frac{\gamma}{2}\hat{p} + \hat{F}_p(t),$$

$$\dot{\hat{x}} = \frac{\hat{p}}{m}, \tag{3.1}$$

where $\kappa$ and $\kappa_3$ are the cavity mode loss of optomechanical and auxiliary cavities, respectively. $\gamma$ is the dissipation rate of the nanosphere motion. $\hat{a}_{\text{in},1}$, $\hat{a}_{\text{in},2}$, and $\hat{a}_{\text{in},3}$ are the input vacuum noise operators, which have zero mean values and obey the nonzero correlation functions given [112],

$$\langle\hat{a}_{\text{in},i}(t)\hat{a}_{\text{in},i}^\dagger(t')\rangle = \delta(t - t'), \tag{3.2}$$

$$\langle\hat{a}_{\text{in},i}^\dagger(t)\hat{a}_{\text{in},i}(t')\rangle = 0, \tag{3.3}$$

where $i = 1,2,3$. $\hat{F}_p(t)$ is the noise force, which obeys the general correlation function as in Ref. [113]. For the optically levitated nanosphere, the source of the noise force mainly contains shot noise, blackbody radiation, sphere anisotropy, collisions with a background gas, and momentum recoil kicks due to scattered photons. We can ignore the contributions from the first three aspects for the high mechanical quality of the levitated nanosphere and good vacuum condition. So the correlation function of the noise force depends on the leftover two aspect, and the correlation can be approximated to

$$\langle\hat{F}_p(t)\hat{F}_p(t')\rangle = \phi\omega_m\delta(t - t'). \tag{3.4}$$

Here, $\phi$ is the strength of photon recoil heating and $\omega_m$ is the harmonic-oscillator frequency of the nanosphere.

Under the condition of strong driving, we can linearize Eq. (3.1) around the steady-state mean values by using the transformation $\hat{a}_1 \to \alpha_1 + a_1$, $\hat{a}_2 \to \alpha_2 + a_2$, $\hat{a}_3 \to \alpha_3 + a_3$, and $\hat{x} \to x_0 + x$, where $\alpha_1$, $\alpha_2$, $\alpha_3$, and $x_0$ are the mean values of the operators and $a_1$, $a_2$, $a_3$, and $x$ are the small fluctuating terms. After segregating the mean values and the fluctuating terms, we obtain the equations for the steady-state expectation values of the nanosphere and cavity field

$$0 = -\frac{\kappa}{2}\alpha_1 - iE_1, \tag{3.5}$$

$$0 = \left[i(\Delta_2 + 2gkx_0) - \frac{\kappa}{2}\right]\alpha_2 - iJ\alpha_3 - iE_2, \tag{3.6}$$

$$0 = \left(i\Delta_3 - \frac{\kappa_3}{2}\right)\alpha_3 - iJ^*\alpha_2 - iE_3, \tag{3.7}$$

$$0 = -4gk^2|\alpha_1|^2x_0 + 2gk|\alpha_2|^2, \tag{3.8}$$

$$0 = p_0. \tag{3.9}$$

In the following derivation, there are some higher-order terms of fluctuation. These terms are much less than the lower terms and have minimal effects on motion equations. On the other hand, they denote the transition process far away from the eigenfrequency of cavity, which has rare probability. It is advisable to ignore these terms. We need a steady potential to trap the nanosphere. The resonant trap pump ($\Delta_1 = 0$) can make the mode 1 form a standard standing wave which insures the spatial distribution of potential is time independent, and then better meets this demand. By neglecting the higher-order terms and choosing $\Delta_1 = 0$, the linear quantum Langevin equations read

$$\dot{a}_1 = -\frac{\kappa}{2}a_1 - i4gk^2x_0\alpha_1x + \sqrt{\kappa}\hat{a}_{\text{in},1}, \tag{3.10}$$

$$\dot{a}_2 = \left[i(\Delta_2 + 2gkx_0) - \frac{\kappa}{2}\right]a_2 + 2ig\alpha_2kx - iJa_3 + \sqrt{\kappa}\hat{a}_{\text{in},2}, \tag{3.11}$$

$$\dot{a}_3 = \left(i\Delta_3 - \frac{\kappa_3}{2}\right)a_3 - iJ^*a_2 + \sqrt{\kappa_3}\hat{a}_{\text{in},3}, \tag{3.12}$$

$$\dot{p} = -4gk^2|\alpha_1|^2x - \frac{\gamma}{2}p + \hat{F}_p(t) + 2gk[\alpha_2a_2^\dagger + \alpha_2^*a_2 - 2kx_0(\alpha_1a_1^\dagger + \alpha_1^*a_1)], \tag{3.13}$$

$$\dot{x} = \frac{p}{m}. \tag{3.14}$$

From Eq. (3.13), we note that cavity mode 1 provides a linear restoring force $-4gk^2|\alpha_1|^2x$ which is equivalent to $-m\omega_m^2x$. The corresponding linearized system Hamilton is written as

$$H = -\Delta_1a_1^\dagger a_1 - \Delta_2'a_2^\dagger a_2 - \Delta_3a_3^\dagger a_3 + \frac{p^2}{2m} + 4gk^2|\alpha_1|^2x^2 - (\Omega_ma_2^\dagger + \Omega_m^*a_2)(b^\dagger + b) + Ja_2^\dagger a_3 + J^*a_3^\dagger a_2, \tag{3.15}$$

where $\Delta_2' = \Delta_2 + 2gkx_0$ is the detuning relative to the new resonance frequency of the optomechanical cavity, $b$ is the annihilation operator of the mechanical mode which has expression $\frac{x}{x_{\text{ZPF}}} + i\frac{p}{\sqrt{2m\hbar\omega_m}}$, and $\Omega_m$ is the effective optomechanical coupling strength which is defined as $\Omega_m = 2gkx_{\text{ZPF}}\alpha_2$. Here $x_{\text{ZPF}}$ is the zero-point fluctuation of the nanosphere with expression $\sqrt{\hbar/2m\omega_m}$.

The energy levels for the linearized Hamiltonian are demonstrated in Fig. 2(a). The transition processes among levels contain two parts. The primary one is the cooling and heating processes on account of the interaction between the cooling optical mode and the nanosphere in the optomechanical cavity [7,114], which are denoted by the one-way arrows. The other is the energy swapping of the optomechanical and the auxiliary cavities due to the tunneling between them, which is labeled by the red double arrows. Because the new energy level and new transition are added, the certain combination transition of the system is similar to a three-level system. Thus a quantum interference like the three-level system will be generated.

In our work, we focus on the heating transition process $|n_2,n_3,m\rangle \to |n_2 + 1,n_3,m + 1\rangle$. From Fig. 2(b), we can see that there are two different excitation pathways to realize this process. The one is $|0\rangle \to |1\rangle$, which is taken charge by the term $\Omega_ma_2^\dagger b^\dagger$ in Hamilton Eq. (3.15); the other one is
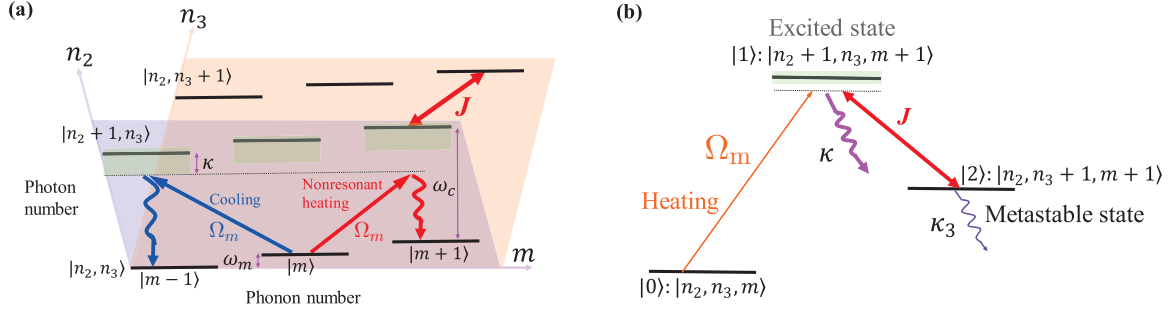
FIG. 2. (a) Energy-level diagram of the linearized Hamiltonian [see Eq. (3.15)]. Here $|n_2,n_3,m\rangle$ denotes the state for $n_2$ number cooling field photons in the optomechanical cavity, $n_3$ number photons in auxiliary cavity, and $m$ number phonons in mechanical mode of the nanosphere. The one-way arrows represent the cooling (blue arrows) and heating (red arrows) processes due to sideband resonance. The transition between energy levels of two coupled cavities is denoted by red double arrow. (b) The three-level configuration extracted from Fig. 2(a). State $|1\rangle$ stands for a short-lived state with high decay rate $\kappa$ and $|2\rangle$ represents a long-lived metastable state with small decay rate $\kappa_3$. It should be pointed out emphatically that the levels $|n_2 + 1,n_3\rangle$ and $|n_2,n_3 + 1\rangle$ have obvious interval in this figure, but they are degenerate.

$|0\rangle \rightarrow |1\rangle \rightarrow |2\rangle \rightarrow |1\rangle$, which is taken charge by the terms $\Omega_m a_2^\dagger b^\dagger + J a_2^\dagger a_3 + J^* a_3^\dagger a_2$ in Hamilton Eq. (3.15). These two pathways are indistinguishable, and then cause the destructive quantum interference which is similar to the EIT effect. Therefore, the excitation channel $|0\rangle \rightarrow |1\rangle$ is suppressed and a lower cooling limit is obtained.

## IV. COOLING OF NANOSPHERE

### A. Optical force spectrum

From the interaction term between optical mode 2 and the center-of-mass motion of nanosphere in Eq. (3.15), we can derive the optical force on the nanosphere

$$F = (\Omega_m a_2^\dagger + \Omega_m^* a_2)/x_{\text{ZPF}}. \quad (4.1)$$

By the Fourier transformation of the correlation function, the corresponding quantum noise spectrum is expressed as

$$S_{FF}(\omega) \equiv \int \langle F(t)F(0)\rangle e^{i\omega t} dt. \quad (4.2)$$

To gain the analytic expression of this noise spectrum, we treat the optomechanical coupling as a perturbation to the optical field because of the strong dissipative nature of the optomechanical cavity. First, we transform the corresponding linear motion equations to the frequency domain, i.e.,

$$-i\omega \tilde{a}_2(\omega) = \left(i\Delta_2' - \frac{\kappa}{2}\right)\tilde{a}_1(\omega) + i\Omega_m[\tilde{b}^\dagger(\omega) + \tilde{b}(\omega)]$$
$$- iJ\tilde{a}_3(\omega) + \sqrt{\kappa}\tilde{a}_{\text{in},2}(\omega), \quad (4.3)$$

$$-i\omega \tilde{a}_3(\omega) = \left(i\Delta_3 - \frac{\kappa_3}{2}\right)\tilde{a}_3(\omega) - iJ^*\tilde{a}_2(\omega) + \sqrt{\kappa_3}\tilde{a}_{\text{in},3}(\omega), \quad (4.4)$$

$$-i\omega \tilde{b}(\omega) = \left(-i\omega_m - \frac{\gamma}{2}\right)\tilde{b}(\omega) + i[\Omega_m\tilde{b}^\dagger(\omega) + \Omega_m^*\tilde{b}(\omega)]$$
$$+ \sqrt{\gamma}\tilde{b}_{in}(\omega). \quad (4.5)$$

Then we derive the expression for $\tilde{b}(\omega)$ as

$$\tilde{b}(\omega) \simeq \frac{\sqrt{\gamma}\tilde{b}_{in}(\omega) + i\sqrt{\kappa}A_2(\omega) + \sqrt{\kappa_3}A_3(\omega)}{i\omega - i[\omega_m + \Sigma(\omega)] - \frac{\gamma}{2}}, \quad (4.6)$$

where

$$A_2(\omega) = \Omega_m^* \chi(\omega)\tilde{a}_{\text{in},2}(\omega) + \Omega_m \chi^*(-\omega)\tilde{a}_{\text{in},2}^\dagger(\omega), \quad (4.7)$$

$$A_3(\omega)=J[\Omega^*\chi(\omega)\chi_3(\omega)\tilde{a}_{\text{in},3}(\omega) - \Omega\chi^*(-\omega)\chi_3^*(-\omega)\tilde{a}_{\text{in},3}^\dagger(\omega)], \quad (4.8)$$

$$\Sigma(\omega) = -i|\Omega_m|^2[\chi(\omega) - \chi^*(\omega)], \quad (4.9)$$

$$\chi_2(\omega) = \frac{1}{-i(\omega + \Delta_2') + \kappa/2}, \quad (4.10)$$

$$\chi_3(\omega) = \frac{1}{-i(\omega + \Delta_3) + \kappa_3/2}, \quad (4.11)$$

$$\chi(\omega) = \frac{1}{\frac{1}{\chi_2(\omega)} + |J|^2\chi_3(\omega)}, \quad (4.12)$$

$$\chi_m(\omega) = \frac{1}{-i(\omega - \omega_m) + \gamma/2}. \quad (4.13)$$

Here the effect of the optomechanical and the auxiliary cavities is represented by $A_{2,3}(\omega)$. $\Sigma(\omega)$ accounts for the optomechanical self-energy; $\chi(\omega)$ is the total response function of two coupled cavities and $\chi_2(\omega)$, $\chi_3(\omega)$, and $\chi_m(\omega)$ are the response function of the optomechanical cavity, the auxiliary cavity, and the mechanical mode, respectively. The influence of the optomechanical coupling on the nanosphere motion is the modification of its mechanical frequency $\delta\omega_m = \text{Re}\,\Sigma(\omega_m)$ and damping $\Gamma_{\text{opt}} = -2\,\text{Im}\,\Sigma(\omega_m)$.

With the above preparation, we obtain the spectral density for the optical force:

$$S_{FF}(\omega) = \frac{|\Omega_m\chi(\omega)|^2}{x_{\text{ZPF}}^2}[\kappa + \kappa_3|J|^2|\chi_3(\omega)|^2]. \quad (4.14)$$

For a general cavity optomechanical system, the noise spectrum has the form of $S_{FF}(\omega) = |\Omega_m\chi_2(\omega)|^2\kappa/x_{\text{ZPF}}^2$, which equals to Eq. (4.14) choosing $J = 0$. This is a typical Lorentzian line shape. From Eq. (4.14), it can be observed that
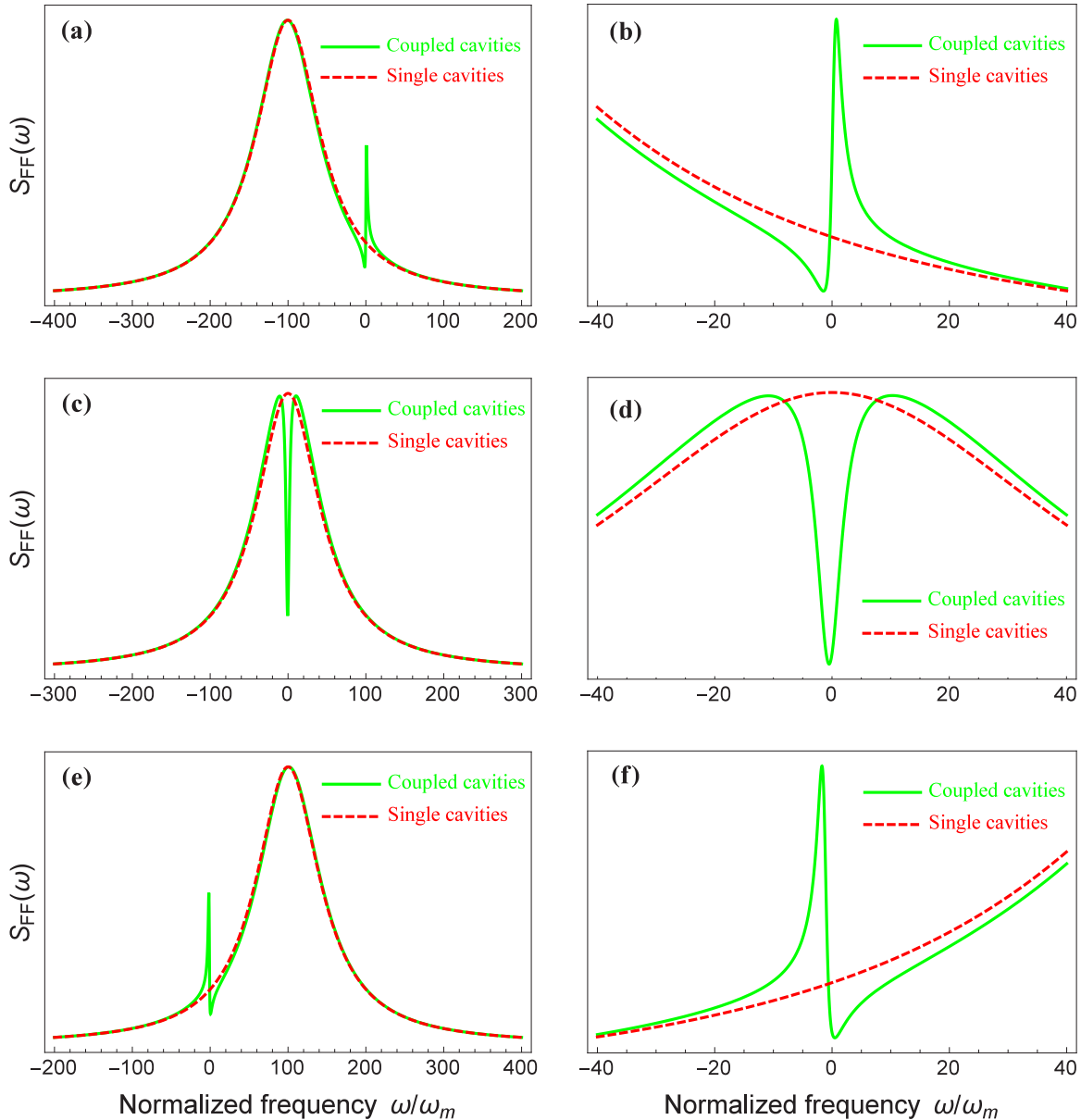
FIG. 3. Optical force spectrum $S_{FF}(\omega)$ of the single cavity and coupled cavities vs normalized frequency $\omega/\omega_m$ for various normalized detuning $\Delta_2'/\omega_m$. The quantities $S_{FF}(\omega)$ and $\omega/\omega_m$ are dimensionless. (a) The spectrum for blue detuning $\Delta_2' = 100\omega_m$. (b) Detailed view of (a) for Fano line shape. (c) The spectrum for resonant $\Delta_2' = 0$. (d) Detailed view of (c) for EIT-like line shape. (e) The spectrum for red detuning $\Delta_2' = -100\omega_m$. (f) Detailed view of (e) for Fano line shape. The other parameters are $\Delta_3 = 0.5\omega_m$, $\kappa/\omega_m = 100$, $\kappa_3 = \omega_m$, $J = \sqrt{\kappa\omega_m}$, $\Omega_m = 5\omega$, and $\gamma = 10^{-5}\omega_m$.

the spectral density of a coupling cavities system has a complex modification compared to a single cavity. The modification contains the information of cavity mode 3. This means that the optical force on the nanosphere is relative to mode 3, i.e., there is nondirect interaction between the nanosphere and the mode 3. We will discuss this interaction in Sec. V A in detail.

The spectral density of the optical force $S_{FF}(\omega)$ for both single cavity and coupled cavities with different types of detuning values in the unresolved-sideband are depicted in Fig. 3. From Figs. 3(a), 3(c) and 3(e), one finds that the noise spectra of the single cavity and the coupled cavities are identical in the range far away from the resonant region of the auxiliary cavity, while a new line shape appears in the resonant region of the auxiliary cavity for a coupled cavities system. The feature of new resonance peaks in Figs. 3(b), 3(d) and 3(f) is related to the position of the resonant regions of the optomechanical and the auxiliary cavities. When the resonant regions are separate, the line shape of the new resonance peaks is an asymmetric Fano line shape [64,90,115], as shown in Figs. 3(b) and 3(f). And for the overlapping case, i.e., $\Delta_2' \simeq \Delta_3$, the line shape is a symmetric EIT-like line shape. The emergence of a new line shape changes the symmetry of the background with symmetric Lorentzian line shape.

The transition process in dynamics inevitably accompanies the absorption and emission of certain frequency photons. Consequently, the enhancement or suppression of the transition
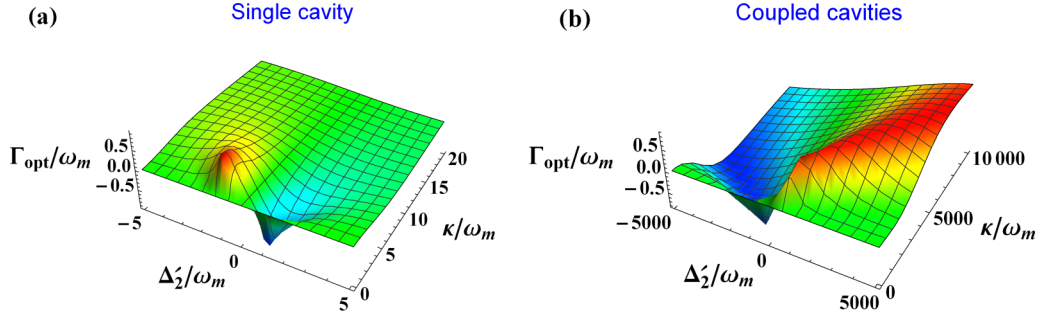
FIG. 4. Net cooling rate $\Gamma_{\text{opt}}$ as functions of normalized detuning $\Delta_2'/\omega_m$ and normalized decay rate $\kappa/\omega_m$ for a single cavity (a) and coupled cavities (b). The quantities $\Gamma_{\text{opt}}/\omega_m$, $\Delta_2'/\omega_m$, and $\kappa/\omega_m$ are dimensionless. The relevant parameters are $\Delta_3 = 0.5\omega_m$, $\kappa_3 = \omega_m$, $J = \sqrt{\kappa\omega_m}$, $\Omega_m = \omega/4$, and $\gamma = 10^{-5}\omega_m$.

process owing to the quantum interference has great influence on the absorption and emission of certain frequency photons. The direct reflection is that a sharp peak or valley shows up in the smooth absorption spectrum of the system. According to the expression of the optical force on the nanosphere Eq. (4.1), it is clear that the optical force spectrum essentially reflects the absorption property of the cooling optical mode 2. So the sharp peak or valley in Fig. 3 presents the enhancing or suppression of the absorption of certain frequency photons caused by the quantum interference. The frequency corresponding to the valley is the certain frequency relative to the interference transition process.

So, it is a decent approach for a preferable cooling performance that the interference can be utilized by adjusting the optical parameter of the system to suppress the heating effect and enhance the cooling one.

### B. Cooling rate

For our system, the cooling and heating rates $A_\mp$ are given by

$$A_\mp = S_{FF}(\pm\omega_m)x_{\text{ZPF}}^2. \tag{4.15}$$

The net cooling rate is defined as

$$\Gamma_{\text{opt}} = A_- - A_+. \tag{4.16}$$

In Figs. 4(a) and 4(b), we plot the net cooling rate for the single cavity and coupled cavities systems. There are two discrepancies between them. For the coupled cavities, the optimum cooling detuning is blue and the high cooling rate widely appears at the region of larger decay rate. Due to the existence of the auxiliary cavity, the effective detuning of the nanosphere cooling dynamics is no longer $\Delta_2'$. So $\Delta_2' < 0$ is not the appropriate choice for the nanosphere cooling. The details will be discussed in Sec. V A. When the coupled cavities system is in the cooling regime, the cooling rate $A_-$ is unchanged while the heating rate $A_+$ is largely suppressed on account of the quantum interference. Consequently, a large net cooling rate is gained. The larger the damping, the more apparently the auxiliary cavity modifies the symmetry between heating and cooling processes for extensive detuning. So a large net cooling rate for a wide range is shown.

### C. Cooling limit

The steady-state cooling limit (i.e., the final mean photon number) of the coupled cavities is similar to the single cavity [6], which reads

$$n_f = \frac{A_+ + \gamma_{\text{sc}}}{\Gamma_{\text{opt}}}. \tag{4.17}$$

The cooling limit consists of two parts. $n_f^q = A_+/\Gamma_{\text{opt}}$ is the quantum limit of cooling which relates to the quantum backaction. The classic cooling limit $n_f^c = \gamma_{\text{sc}}/\Gamma_{\text{opt}}$ is tied to the specific conditions of a particular system.

According to the above analysis, we know the quantum interference suppresses the heat rate $A_+$ in connection with the quantum backaction heating and gives rise to a larger net cooling rate $\Gamma_{\text{opt}}$. As a result, the coupled cavities system has much smaller quantum limit of cooling $n_f^q$ than the single one. With the same physical quantity $\gamma_{\text{sc}}$ in both the single cavity and the coupled cavities systems, the classic cooling limit $n_f^c$ is much smaller in the coupled cavities system due to the large net cooling rate $\Gamma_{\text{opt}}$. To recap, the coupled cavities system can achieve ground-state cooling in an extensive range of parameters. In the following, a set of experimentally plausible parameters are adopted by reference to the related experiments [7,51,56,62] to show this result. We consider a silica sphere with radius $r = 50$ nm and mechanical frequency $\omega_m/(2\pi) = 0.5$ MHz is levitated inside a cavity with $L = 1$ cm and waist $w = 25$ $\mu$m. The wavelength of the trap laser is taken $\lambda = 1$ $\mu$m and the material properties $\epsilon = 2$. Specifically, we take the effective optomechanical coupling strength $\Omega_m/\omega_m = 1/4 < 1$ for ensuring the validity of the perturbative result. This means the coupling between the cavity mode 2 and the nanosphere is weaker than the frequency of the nanosphere, which is different from the relevant study [90,96]. Besides, the influence originating from the background gas can be negligible.

The effect of the tunneling strength $J$ on the cooling limit is shown in Fig. 5(a). We find that the ground-state cooling can be achieved for a wide range of larger tunneling strengths. More carefully, the significant effect occurs at a narrow region of the effective tunneling strength increasing from zero; meanwhile, the cooling limit hardly changes for enlarging the strength as the limit attains a certain value. This means the auxiliary cavity has a limit work for the nanosphere cooling. In Fig. 5(b), we demonstrate the steady-state cooling
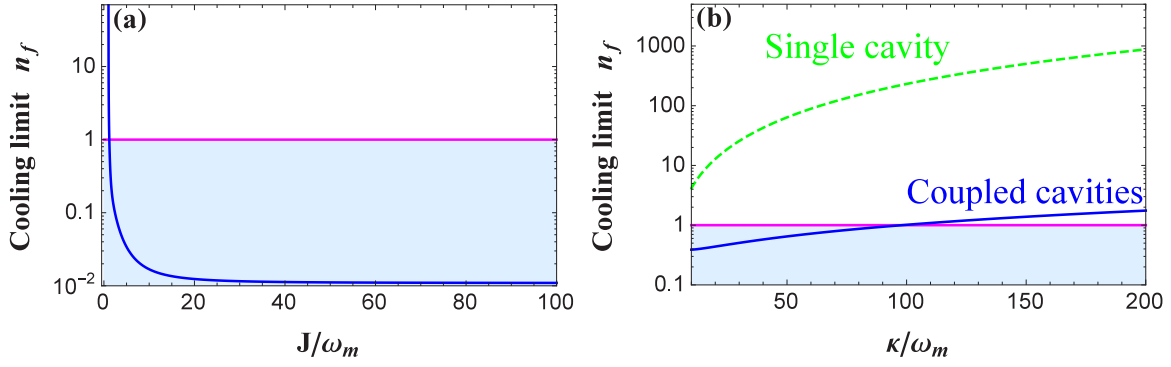
FIG. 5. Steady-state cooling limit as a function of (a) the various normalized coupling strength $J/\omega_m$ and (b) the various normalized damping $\kappa/\omega_m$ for the single cavity and coupled cavities. The quantities $n_f$, $J/\omega_m$, and $\kappa/\omega_m$ are dimensionless. For (a), the detuning $\Delta_2' = \omega_m$ and the decay rate $\kappa/\omega_m = (J/\omega)^2$. In (b), the solid blue line denotes the final phonon number of the nanosphere for coupled cavities. Meanwhile, the dashed green line stands for the single cavity. The shaded region denotes $n_f < 1$. The optimum detuning $\Delta_2' = J^2/(\Delta_3 + \omega_m)$ is in accordance with Ref. [96] and $J = \sqrt{\kappa \omega_m}$. The other parameters are $\Delta_3 = 0.5\omega_m$, $\kappa_3 = \omega_m$, $\gamma = 10^{-5}\omega_m$, and $\Omega_m = \omega_m/4$. For the nanosphere, the radius is chosen as $r = 50$ nm and the operating wavelength is taken as $\lambda = 1$ $\mu$m.

limit of the single cavity and coupled cavities for the various normalized damping $\kappa/\omega_m$. As shown in Fig. 5(b), the single cavity system in the unresolved-sideband regime ($\kappa/\omega_m \gg 1$) is not able to cool the nanosphere to the ground state. For the coupled cavities, due to the quantum interference originating from the addition of the auxiliary cavity, ground-state cooling can be achieved for a larger range of normalized damping $\kappa/\omega_m$.

The physical quantity $\gamma_{sc}$ in the classic cooling limit is characterized by the nanosphere volume $V$ under the condition of the same material and trap field since $\gamma_{sc} = \omega_m \frac{4\pi^2}{5} \frac{\epsilon-1}{\epsilon+2}(V/\lambda^3)$ [7]. The decay rate of the auxiliary cavity influences the optomechanical response of the nanosphere, and then changes the cooling limit of the nanosphere. For these reasons, the radius of the nanosphere related to the nanosphere volume and the damping rate of the auxiliary cavity are crucial parameters in the coupled-cavity-nanosphere system. Figure 6 shows the influence of them on the cooling limit. Figure 6(a) plots the cooling limit as a function of normalized damping $\kappa/\omega_m$ for different radii of the nanosphere. One finds that the cooling limit is not sensitive to the size of the nanosphere when the decay rate $\kappa$ is small. The size of the nanosphere largely affects the cooling limit in the large decay rate $\kappa$ regime and the nanosphere with smaller radius can achieve the ground-state cooling in a wide range of the parameter $\kappa$. When $\kappa$ is large, the increase of the nanosphere radius will change the physical quantity $\gamma_{sc}$ rapidly, so the classic cooling limit increases too rapidly to remain the nanosphere in the ground-state regime. Figure 6(b) plots the cooling limit as a function of normalized auxiliary cavity damping $\kappa_3/\omega_m$ for different decay rates $\kappa$. It is demonstrated that the system can realize ground-state cooling in a wide range of parameter $\kappa$ under the condition $\kappa_3/\omega_m < 1$, and the cooling limit is sensitive to the decay rate $\kappa$ for $\kappa_3/\omega_m > 1$. It is more difficult to achieve ground-state cooling for larger $\kappa$ in the range of $\kappa_3/\omega_m > 1$. The quantum interference leads to the actual damping of the hybrid system to relate to $\kappa_3$. When $\kappa_3/\omega_m < 1$, the hybrid system is actually in a resolved regime and ground-state cooling can be obtained easily, but for $\kappa_3/\omega_m > 1$, one would obtain the opposite result (see Sec. V A for details).

## V. DISCUSSION

From the above study, we know that the auxiliary cavity not only changes the symmetry between the heating and cooling processes of the nanosphere, but also modifies the cooling dynamics of the nanosphere. There exists indirect interaction between the cavity mode $a_3$ and the nanosphere. For the sake of understanding the corresponding result, we will derive the effective parameters for the coupled cavities and discuss the dynamical stability condition of our model in this section.

### A. Effective coupling

The current system is in the highly unresolved regime $\kappa \gg \omega_m$. The coupling between the cavity mode $a_2$ and the nanosphere is weak ($\Omega_m \ll \omega_m$), which can be taken as a perturbation. Therefore, the analytical dynamical equations can be derived only for the cavity mode $a_3$ and the nanosphere. For Eqs. (3.9), (3.10), and (3.12), we derive the formal solution of the corresponding operators by formal integration:

$$a_2 = a_2(0)e^{i\Delta_2' t - \frac{\kappa}{2}t} + e^{i\Delta_2' t - \frac{\kappa}{2}t}\int_0^t [2ig\alpha_2 kx(\tau) - iJa_3(\tau)$$
$$+ \sqrt{\kappa}a_{\text{in},2}(\tau)]e^{-i\Delta_2'\tau + \frac{\kappa}{2}\tau}d\tau, \quad (5.1)$$

$$a_3 = a_3(0)e^{i\Delta_3 t - \frac{\kappa_3}{2}t} + e^{i\Delta_3 t - \frac{\kappa_3}{2}t}\int_0^t [-iJ^*a_2(\tau)$$
$$+ \sqrt{\kappa_3}a_{\text{in},3}(\tau)]e^{-i\Delta_3\tau + \frac{\kappa_3}{2}\tau}d\tau, \quad (5.2)$$

$$x = \frac{p}{m}t + \int_0^t F_x(\tau)d\tau. \quad (5.3)$$

Because $\kappa \gg J$ and $g \ll \omega_m$, we neglect the corresponding terms and obtain

$$a_3 = a_3(0)e^{i\Delta_3 t - \frac{\kappa_3}{2}t} + A_{\text{in},3}(t), \quad (5.4)$$

$$x = \frac{p}{m}t + F_X(t), \quad (5.5)$$

where $A_{\text{in},3}(t)$ and $F_X(t)$ represent the noise terms. Plugging Eqs. (5.4) and (5.5) into Eq. (5.1) under the condition $|\Delta_2'| \gg$
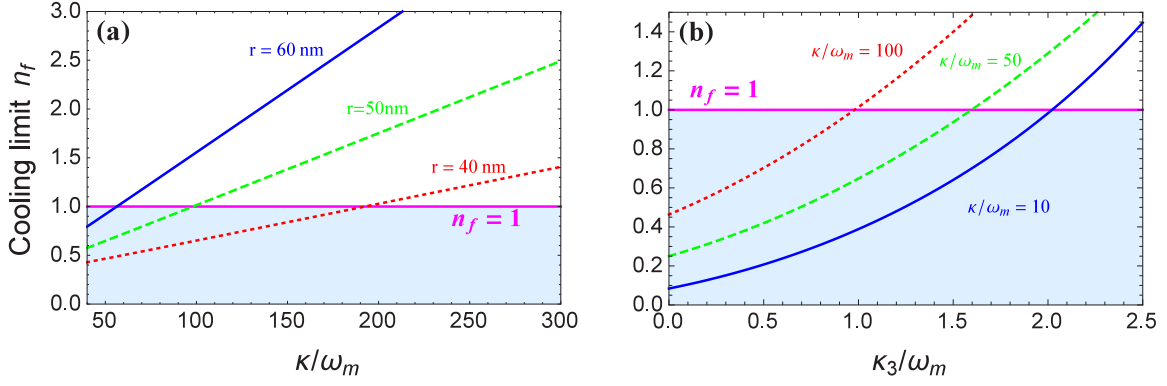
FIG. 6. Cooling limit as functions of normalized damping $\kappa/\omega_m$ for different radius of the nanosphere with $\kappa_3 = \omega_m$ (a) and normalized auxiliary cavity damping $\kappa_3/\omega_m$ for different normalized decay rate $\kappa/\omega_m$ with $r = 50$ nm (b). The quantities $n_f$, $\kappa/\omega_m$, and $\kappa_3 = \omega_m$ are dimensionless. The shaded region denotes $n_f < 1$. The relevant parameters are $\Delta_3 = 0.5\omega_m$, $\Delta_2' = J^2/(\Delta_3 + \omega_m)$, $J = \sqrt{\kappa\omega_m}$, $\Omega_m = \omega/4$, and $\gamma = 10^{-5}\omega_m$.

$|\Delta_3|, \kappa \gg (\kappa_3, \gamma)$, we have

$$a_2 = a_2(0)e^{i\Delta_2' t - \frac{\kappa}{2}t} + \frac{2ig\alpha_2 kx(t)}{-i\Delta_2' + \frac{\kappa}{2}} - \frac{iJa_3(t)}{-i\Delta_2' + \frac{\kappa}{2}} + A_{\mathrm{in},2}(t). \quad (5.6)$$

Substituting Eq. (5.6) into Eqs. (3.10) and (3.12) and neglecting the terms containing $e^{-\frac{\kappa}{2}t}$, one can compare the equations with the single cavity case and then derive

$$i\Delta_3 - \frac{\kappa_3}{2} + \frac{|J|^2}{i\Delta_2' - \frac{\kappa}{2}} \longleftrightarrow i\Delta_{\mathrm{eff}} - \frac{\kappa_{\mathrm{eff}}}{2}, \quad (5.7)$$

$$\left| \frac{J^*\Omega_m}{i\Delta_2' - \frac{\kappa}{2}} \right| \longleftrightarrow |\Omega_{m\mathrm{eff}}|, \quad (5.8)$$

where $|\Omega_{m\mathrm{eff}}| = \eta|\Omega_m|$, $\kappa_{\mathrm{eff}} = \kappa_3 + \eta^2\kappa$, $\Delta_{\mathrm{eff}} = \Delta_3 - \eta^2\Delta_2'$, and $\eta = \frac{|J|}{[\Delta_2'^2 + (\frac{\kappa}{2})^2]^{\frac{1}{2}}}$.

Therefore, we reduce a three-mode system to a two-mode system [96]. For the effective detuning $\Delta_{\mathrm{eff}}$, because the detuning $\Delta_3$ is greater than zero and small as the system at cooling state, only $\Delta_2' \gg 0$ (i.e., the detuning is blue) can make $\Delta_{\mathrm{eff}} < 0$ be in the optimum detuning regime. Under the condition of $\kappa \gg J$, the parameter $\eta$ is far less than 1, so the effective decay rate $\kappa_{\mathrm{eff}} \simeq \kappa_3$. This means that the indirect coupling can bring the system from high unresolved regime to an effective resolved regime and explain why the actual damping of the hybrid system is only related to $\kappa_3$.

So, the real physical process of our model is modulating the property of a cooling optical mode in an optomechanical cavity by the direct coupling between the optomechanical and the auxiliary cavity, and then modulating the property of the optical force on nanosphere through the direct coupling between the cooling optical mode and the nanosphere. If we eliminate the medium role of the cooling optical mode, one can see that there is indirect coupling between the auxiliary cavity and the nanosphere, i.e., the final result is equivalent to using the optical mode 3 in the auxiliary cavity to cooling the nanosphere.

### B. Dynamical stability condition

The dynamical stability condition of the system is derived by the Routh-Hurwitz criterion [116]. For the single cavity system, the dynamical stability condition reads

$$\Delta_2' \left[ 16\Delta_2'|\Omega_m|^2 + \left(4\Delta_2'^2 + \kappa^2\right)\omega_m \right] < 0. \quad (5.9)$$

When the system is in the resolved regime, the detuning for the optimum cooling limit is $\Delta_2' = -\kappa/2$. Thus Eq. (5.9) is simplified as

$$|\Omega_m|^2 < \frac{\kappa\omega_m}{4}. \quad (5.10)$$

The dynamical stability condition for the coupled cavities is given in terms of the derived effective parameters

$$\Delta_{\mathrm{eff}} \left[ 16\Delta_{\mathrm{eff}}|\Omega_{m\mathrm{eff}}|^2 + \left(4\Delta_{\mathrm{eff}}^2 + \kappa_{\mathrm{eff}}^2\right)\omega_{m\mathrm{eff}} \right] < 0. \quad (5.11)$$

Similarly, we take the effective detuning $\Delta_{\mathrm{eff}} = -\omega_m$ which is the optimum detuning for effective optomechanical interaction in the resolved regime. Then Eq. (5.11) reduces to

$$|\Omega_{m\mathrm{eff}}|^2 < \omega_m^2/4 + \kappa_{\mathrm{eff}}^2/16. \quad (5.12)$$

Back to real parameters, we have

$$|\Omega_m|^2 < \frac{4\omega_m^2 + (\kappa_3 + \eta^2\kappa)^2}{16\eta^2}. \quad (5.13)$$

For Eq. (5.13), when $\eta = \eta_{\min} \equiv \sqrt[4]{4\omega_m^2 + \kappa_3^2}/\sqrt{\kappa}$, the right of it has minimum $S_{\min} = \frac{\kappa}{4}\sqrt{\omega_m^2 + \frac{\kappa_3^2}{4}} + \frac{\kappa\kappa_3}{8}$. Comparing $S_{\min}$ with the right of Eq. (5.10), one finds that $S_{\min}$ is larger than the right of Eq. (5.10). It indicates that, in comparison to the single cavity, the coupled cavities system tolerates a larger optomechanical coupling to keep the system in a stable regime.

### VI. CONCLUSION

In conclusion, we have theoretically investigated the ground-state cooling of an optically levitated nanosphere in the highly unresolved regime by introducing a coupled cavity. The auxiliary cavity is coupled with the optomechanical cavity, but does not interact with the levitated nanosphere. This specific configuration of energy transition causes the quantum

interference, which modifies the optomechanical response of the nanosphere and gives rise to asymmetry between heating and cooling processes. By tuning the detuning between an optomechanical cavity and a cooling field, one can take advantage of this interference to enhance the cooling process and restrain the heating process, so that a larger net cooling rate is obtained in a wide range of parameters and the cooling limit is lowered dramatically. When the frequency of an oscillator is a definite value, the coupled system can make the tolerance of the cavity mode loss for the ground-state cooling increase several orders of magnitude more than the single one. An equivalent case is that the coupled system greatly reduces the cooling frequency of an oscillator for a definite cavity loss. This means the coupled system can realize ground-state cooling of low oscillation frequency with large cavity decay. It is found that ground-state cooling can still be achieved for large optomechanical cavity decay rate $\kappa$ even if the effective optomechanical coupling $\Omega_m$ is weaker than the frequency of the nanosphere $\omega_m$. The cooling limit in our research is sensitive to the radius of the nanosphere as well as the damping rate of the auxiliary cavity. The increase of nanosphere radius will made the classic cooling limit increase too suddenly to remain the nanosphere in ground-state regime. The larger the decay rate of the auxiliary cavity, the smaller the optomechanical cavity dissipation that the ground-state cooling can tolerate. The effective interaction between the auxiliary cavity and the levitated nanosphere brings the system from the highly unresolved-sideband regime

to an effective resolved-sideband regime. This significantly relaxes the restricted condition that the system must be in the resolved-sideband regime for the nanosphere cooling. Furthermore, the interaction refines the dynamical stability compared to the case without the auxiliary cavity. This means that the coupled cavities system can keep the cooling state for a wider range of parameters than the single cavity system.

Experimentally, it is a mature technology that ultrasmall-volume cavities can be engineered to have an ultrahigh optical quality factor $Q$ in photonic crystal by adding defects [97,98,117]. Meanwhile the optomechanical experiment can be performed in such a system. And many experiments containing two coupled cavities in photonic crystals have observed the quantum interference effect which is similar to our model [109,118,119]. The latest research suggests that the nanosphere can be optically trapped and controlled inside evacuated hollow core photonic crystal fibers [120,121]. So the model we propose can be experimentally realized if we integrate the process of the three points above. This work may provide the possibility for the corresponding research and application of the levitated nanosphere system beyond the restriction for the current experiment.

[1] I. Wilson-Rae, N. Nooshi, W. Zwerger, and T. J. Kippenberg, Phys. Rev. Lett. **99**, 093901 (2007).

[2] F. Marquardt, J. P. Chen, A. A. Clerk, and S. M. Girvin, Phys. Rev. Lett. **99**, 093902 (2007).

[3] T. J. Kippenberg and K. J. Vahala, Opt. Express **15**, 17172 (2007).

[4] T. Kippenberg and K. Vahala, Science **321**, 1172 (2008).

[5] F. Marquardt and S. Girvin, Physics **2**, 40 (2009).

[6] M. Aspelmeyer, T. J. Kippenberg, and F. Marquardt, Rev. Mod. Phys. **86**, 1391 (2014).

[7] D. E. Chang, C. A. Regal, S. B. Papp, D. J. Wilson, O. Painter, H. J. Kimble, and P. Zoller, Proc. Natl. Acad. Sci. USA **107**, 1005 (2010).

[8] O. Romero-Isart, A. C. Pflanzer, M. L. Juan, R. Quidant, N. Kiesel, M. Aspelmeyer, and J. I. Cirac, Phys. Rev. A **83**, 013803 (2011).

[9] T. S. Monteiro, J. Millen, G. A. T. Pender, F. Marquardt, D. Chang, and P. F. Barker, New J. Phys. **15**, 015001 (2013).

[10] Z.-Q. Yin, A. A. Geraci, and T. C. Li, Int. J. Mod. Phys. B **27**, 1330018 (2013).

[11] L. P. Neukirch and A. N. Vamivakas, Contemp. Phys. **56**, 48 (2015).

[12] D. W. Vernooy, V. S. Ilchenko, H. Mabuchi, E. W. Streed, and H. J. Kimble, Opt. Lett. **23**, 247 (1998).

[13] K. G. Libbrecht and E. D. Black, Phys. Lett. A **321**, 99 (2004).

[14] A. A. Geraci, S. B. Papp, and J. Kitching, Phys. Rev. Lett. **105**, 101101 (2010).

[15] A. Arvanitaki and A. A. Geraci, Phys. Rev. Lett. **110**, 071105 (2013).

[16] T. Li, *Fundamental Tests of Physics with Optically Trapped Microspheres* (Springer, New York, 2013).

[17] J. Millen, T. Deesuwan, P. Barker, and J. Anders, Nat. Nanotechnol. **9**, 425 (2014).

[18] D. C. Moore, A. D. Rider, and G. Gratta, Phys. Rev. Lett. **113**, 251801 (2014).

[19] G. Ranjit, D. P. Atherton, J. H. Stutz, M. Cunningham, and A. A. Geraci, Phys. Rev. A **91**, 051805(R) (2015).

[20] J. Li, S. Zippilli, J. Zhang, and D. Vitali, Phys. Rev. A **93**, 050102(R) (2016).

[21] G. Ranjit, M. Cunningham, K. Casey, and A. A. Geraci, Phys. Rev. A **93**, 053801 (2016).

[22] A. D. Rider, D. C. Moore, C. P. Blakemore, M. Louis, M. Lu, and G. Gratta, Phys. Rev. Lett. **117**, 101101 (2016).

[23] J. Liu and K.-D. Zhu, Phys. Rev. D **95**, 044014 (2017).

[24] E. B. Aranas, P. G. Z. Fonseca, P. F. Barker, and T. S. Monteiro, New J. Phys. **18**, 113021 (2016).

[25] A. Xuereb and M. Paternostro, Phys. Rev. A **87**, 023830 (2013).

[26] J. Gieseler, L. Novotny, and R. Quidant, Nat. Phys. **9**, 806 (2013).

[27] J. Gieseler, M. Spasenović, L. Novotny, and R. Quidant, Phys. Rev. Lett. **112**, 103603 (2014).

[28] M. G. Genoni, J. Zhang, J. Millen, P. F. Barker, and A. Serafini, New J. Phys. **17**, 073019 (2015).

[29] W. Ge, B. Rodenburg, and M. Bhattacharya, Phys. Rev. A **94**, 023808 (2016).

[30] P. Z. G. Fonseca, E. B. Aranas, J. Millen, T. S. Monteiro, and P. F. Barker, Phys. Rev. Lett. **117**, 173602 (2016).

[31] M. Rashid, T. Tufarelli, J. Bateman, J. Vovrosh, D. Hempston, M. S. Kim, and H. Ulbricht, Phys. Rev. Lett. **117**, 273601 (2016).

[32] K.-W. Xiao, N. Zhao, and Z.-q. Yin, Phys. Rev. A **96**, 013837 (2017).

[33] J. Gieseler, R. Quidant, C. Dellago, and L. Novotny, Nat. Nanotechnol. **9**, 358 (2014).

[34] J. Gieseler, L. Novotny, C. Moritz, and C. Dellago, New J. Phys. **17**, 045011 (2015).

[35] O. Romero-Isart, A. C. Pflanzer, F. Blaser, R. Kaltenbaek, N. Kiesel, M. Aspelmeyer, and J. I. Cirac, Phys. Rev. Lett. **107**, 020405 (2011).

[36] O. Romero-Isart, Phys. Rev. A **84**, 052121 (2011).

[37] J. Bateman, S. Nimmrichter, K. Hornberger, and H. Ulbricht, Nat. Commun. **5**, 4788 (2014).

[38] D. Goldwater, M. Paternostro, and P. F. Barker, Phys. Rev. A **94**, 010104(R) (2016).

[39] J. Zhang, T. Zhang, and J. Li, Phys. Rev. A **95**, 012141 (2017).

[40] Z.-q. Yin and T. Li, Contem. Phys. **58**, 119 (2017).

[41] T. Li, S. Kheifets, D. Medellin, and M. G. Raizen, Science **328**, 1673 (2010).

[42] T. Li and M. G. Raizen, Ann. Phys. (NY) **525**, 281 (2013).

[43] W. Nie, Y. Lan, Y. Li, and S. Zhu, Phys. Rev. A **86**, 063809 (2012).

[44] W. Nie, Y. Lan, Y. Li, and S. Zhu, Sci. China Phys. Mech. Astron. **57**, 2276 (2014).

[45] A. A. Zabolotskii, J. Exp. Theor. Phys. **123**, 762 (2016).

[46] T. M. Hoang, Y. Ma, J. Ahn, J. Bang, F. Robicheaux, Z.-Q. Yin, and T. Li, Phys. Rev. Lett. **117**, 123604 (2016).

[47] S. Liu, T. Li, and Z.-q. Yin, J. Opt. Soc. Am. B **34**, C8 (2017).

[48] Y. Minowa, Y. Toyota, and M. Ashida, J. Opt. Soc. Am. B **34**, C20 (2017).

[49] P. F. Barker and M. N. Shneider, Phys. Rev. A **81**, 023826 (2010).

[50] T. Li, S. Kheifets, and M. G. Raizen, Nat. Phys. **7**, 527 (2011).

[51] G. A. T. Pender, P. F. Barker, F. Marquardt, J. Millen, and T. S. Monteiro, Phys. Rev. A **85**, 021802(R) (2012).

[52] W. Nie, Y. Lan, Y. Li, and S. Zhu, Phys. Rev. A **88**, 063849 (2013).

[53] Y. Arita, M. Mazilu, and K. Dholakia, Nat. Commun. **4**, 2374 (2013).

[54] P. Mestres, J. Berthelot, M. Spasenović, J. Gieseler, L. Novotny, and R. Quidant, Appl. Phys. Lett. **107**, 151102 (2015).

[55] J. Millen, P. Z. G. Fonseca, T. Mavrogordatos, T. S. Monteiro, and P. F. Barker, Phys. Rev. Lett. **114**, 123602 (2015).

[56] B. Rodenburg, L. P. Neukirch, A. N. Vamivakas, and M. Bhattacharya, Optica **3**, 318 (2016).

[57] M. Frimmer, J. Gieseler, and L. Novotny, Phys. Rev. Lett. **117**, 163601 (2016).

[58] V. Jain, J. Gieseler, C. Moritz, C. Dellago, R. Quidant, and L. Novotny, Phys. Rev. Lett. **116**, 243601 (2016).

[59] Z.-q. Yin, T. Li, and M. Feng, Phys. Rev. A **83**, 013816 (2011).

[60] J. Gieseler, B. Deutsch, R. Quidant, and L. Novotny, Phys. Rev. Lett. **109**, 103603 (2012).

[61] P. Asenbaum, S. Kuhn, S. Nimmrichter, U. Sezer, and M. Arndt, Nat. Commun. **4**, 2743 (2013).

[62] N. Kiesel, F. Blaser, U. Delić, D. Grass, R. Kaltenbaek, and M. Aspelmeyer, Proc. Natl. Acad. Sci. USA **110**, 14180 (2013).

[63] J. D. Teufel, J. W. Harlow, C. A. Regal, and K. W. Lehnert, Phys. Rev. Lett. **101**, 197203 (2008).

[64] F. Elste, S. M. Girvin, and A. A. Clerk, Phys. Rev. Lett. **102**, 207209 (2009).

[65] M. Li, W. H. P. Pernice, and H. X. Tang, Phys. Rev. Lett. **103**, 223901 (2009).

[66] A. Xuereb, R. Schnabel, and K. Hammerer, Phys. Rev. Lett. **107**, 213604 (2011).

[67] T. Weiss and A. Nunnenkamp, Phys. Rev. A **88**, 023850 (2013).

[68] M.-Y. Yan, H.-K. Li, Y.-C. Liu, W.-L. Jin, and Y.-F. Xiao, Phys. Rev. A **88**, 023802 (2013).

[69] Y. Li, L.-A. Wu, and Z. D. Wang, Phys. Rev. A **83**, 043804 (2011).

[70] J.-Q. Liao and C. K. Law, Phys. Rev. A **84**, 053838 (2011).

[71] X. Wang, S. Vinjanampathy, F. W. Strauch, and K. Jacobs, Phys. Rev. Lett. **107**, 177204 (2011).

[72] S. Machnes, J. Cerrillo, M. Aspelmeyer, W. Wieczorek, M. B. Plenio, and A. Retzker, Phys. Rev. Lett. **108**, 153601 (2012).

[73] C. Genes, H. Ritsch, and D. Vitali, Phys. Rev. A **80**, 061803(R) (2009).

[74] K. Hammerer, K. Stannigel, C. Genes, P. Zoller, P. Treutlein, S. Camerer, D. Hunger, and T. W. Hänsch, Phys. Rev. A **82**, 021803(R) (2010).

[75] T. P. Purdy, D. W. C. Brooks, T. Botter, N. Brahms, Z.-Y. Ma, and D. M. Stamper-Kurn, Phys. Rev. Lett. **105**, 133602 (2010).

[76] M. Paternostro, G. De Chiara, and G. M. Palma, Phys. Rev. Lett. **104**, 243602 (2010).

[77] C. Genes, H. Ritsch, M. Drewsen, and A. Dantan, Phys. Rev. A **84**, 051801(R) (2011).

[78] S. Camerer, M. Korppi, A. Jöckel, D. Hunger, T. W. Hänsch, and P. Treutlein, Phys. Rev. Lett. **107**, 223001 (2011).

[79] B. Vogell, K. Stannigel, P. Zoller, K. Hammerer, M. T. Rakher, M. Korppi, A. Jöckel, and P. Treutlein, Phys. Rev. A **87**, 023816 (2013).

[80] W.-j. Gu and G.-x. Li, Phys. Rev. A **87**, 025804 (2013).

[81] F. Bariani, S. Singh, L. F. Buchmann, M. Vengalattore, and P. Meystre, Phys. Rev. A **90**, 033838 (2014).

[82] A. Dantan, B. Nair, G. Pupillo, and C. Genes, Phys. Rev. A **90**, 033820 (2014).

[83] J. S. Bennett, L. S. Madsen, M. Baker, H. Rubinsztein-Dunlop, and W. P. Bowen, New J. Phys. **16**, 083036 (2014).

[84] J. Restrepo, C. Ciuti, and I. Favero, Phys. Rev. Lett. **112**, 013601 (2014).

[85] T. Ojanen and K. Børkje, Phys. Rev. A **90**, 013824 (2014).

[86] Y. Guo, K. Li, W. Nie, and Y. Li, Phys. Rev. A **90**, 053841 (2014).

[87] G. Ranjit, C. Montoya, and A. A. Geraci, Phys. Rev. A **91**, 013416 (2015).

[88] X. Chen, Y.-C. Liu, P. Peng, Y. Zhi, and Y.-F. Xiao, Phys. Rev. A **92**, 033841 (2015).

[89] W. Nie, A. Chen, and Y. Lan, Phys. Rev. A **93**, 023841 (2016).

[90] B. Sarma and A. K. Sarma, Phys. Rev. A **93**, 033845 (2016).

[91] B.-y. Zhou and G.-x. Li, Phys. Rev. A **94**, 033809 (2016).

[92] Y.-C. Liu, Y.-F. Xiao, X. S. Luan, and C. W. Wong, Sci. China-Phys. Mech. Astron. **58**, 1 (2015).

[93] M. Asjad, S. Zippilli, and D. Vitali, Phys. Rev. A **94**, 051801(R) (2016).

[94] K. A. Yasir, L. Zhuang, and W.-M. Liu, Phys. Rev. A **95**, 013810 (2017).

[95] Y.-C. Liu, Y.-W. Hu, C. W. Wong, and Y.-F. Xiao, Chin. Phys. B **22**, 114213 (2013).

[96] Y.-C. Liu, Y.-F. Xiao, X. Luan, Q. Gong, and C. W. Wong, Phys. Rev. A **91**, 033818 (2015).

[97] M. Notomi, E. Kuramochi, and T. Tanabe, Nat. Photon. **2**, 741 (2008).

[98] J. Zheng, Y. Li, M. S. Aras, A. Stein, K. L. Shepard, and C. W. Wong, Appl. Phys. Lett. **100**, 211908 (2012).

[99] C.-H. Bai, D.-Y. Wang, H.-F. Wang, A.-D. Zhu, and S. Zhang, Sci. Rep. **6**, 33404 (2016).

[100] T. Yousif, W. Zhou, and L. Zhou, J. Mod. Opt. **61**, 1180 (2014).

[101] D.-Y. Wang, C.-H. Bai, H.-F. Wang, A.-D. Zhu, and S. Zhang, Sci. Rep. **6**, 38559 (2016).

[102] R. Grimm, M. Weidemüller, and Y. B. Ovchinnikov, Adv. At. Mol. Opt. Phys. **42**, 95 (2000).

[103] I. S. Grudinin, H. Lee, O. Painter, and K. J. Vahala, Phys. Rev. Lett. **104**, 083901 (2010).

[104] I. S. Grudinin and K. J. Vahala, Opt. Express **17**, 14088 (2009).

[105] C. Zheng, X. Jiang, S. Hua, L. Chang, G. Li, H. Fan, and M. Xiao, Opt. Express **20**, 18319 (2012).

[106] B. Peng, Ş. Kayaözdemir, F. Lei, F. Monifi, M. Gianfreda, G. L. Long, S. Fan, F. Nori, C. M. Bender, and L. Yang, Nat. Phys. **10**, 394 (2014).

[107] Q. Xu, S. Sandhu, M. L. Povinelli, J. Shakya, S. Fan, and M. Lipson, Phys. Rev. Lett. **96**, 123901 (2006).

[108] Y.-F. Xiao, M. Li, Y.-C. Liu, Y. Li, X. Sun, and Q. Gong, Phys. Rev. A **82**, 065804 (2010).

[109] Y. Sato, Y. Tanaka, J. Upham, Y. Takahashi, T. Asano, and S. Noda, Nat. Photon. **6**, 56 (2012).

[110] J. Cho, D. G. Angelakis, and S. Bose, Phys. Rev. A **78**, 022323 (2008).

[111] B.-B. Li, Y.-F. Xiao, C.-L. Zou, X.-F. Jiang, Y.-C. Liu, F.-W. Sun, Y. Li, and Q. Gong, Appl. Phys. Lett. **100**, 021108 (2012).

[112] C. W. Gardiner and P. Zoller, *Quantum Noise* (Springer-Verlag, Berlin, 1991).

[113] V. Giovannetti and D. Vitali, Phys. Rev. A **63**, 023812 (2001).

[114] Y.-C. Liu, Y.-F. Xiao, X. Luan, and C. W. Wong, Phys. Rev. Lett. **110**, 153606 (2013).

[115] S. Stassi, A. Chiadò, G. Calafiore, G. Palmara, S. Cabrini, and C. Ricciardi, Sci. Rep. **7**, 1065 (2017).

[116] E. X. DeJesus and C. Kaufman, Phys. Rev. A **35**, 5288 (1987).

[117] S. Fan, Appl. Phys. Lett. **80**, 908 (2002).

[118] Y.-C. Liu, B.-B. Li, and Y.-F. Xiao, Nanophotonics **6**, 789 (2017).

[119] A. H. Safavi-Naeini, T. P. M. Alegre, J. Chan, M. Eichenfield, M. Winger, Q. Lin, J. T. Hill, D. E. Chang, and O. Painter, Nature (London) **472**, 69 (2011).

[120] D. Grass, J. Fesel, S. G. Hofer, N. Kiesel, and M. Aspelmeyer, Appl. Phys. Lett. **108**, 221103 (2016).

[121] D. S. Bykov, S. Xie, R. Zeltner, A. Machnev, G. K. L. Wong, T. G. Euser, and P. S. J. Russell, arXiv:1709.04053.